ACS APPLIED MATERIALS & INTERFACES

Research Article

www.acsami.org

MgO-Decorated Few-Layered Graphene as an Anode for Li-Ion Batteries

Shaikshavali Petnikota,[†,‡] Naresh K. Rotte,[†] M. V. Reddy,*[,‡,§] Vadali V. S. S. Srikanth,*[,†] and B. V. R. Chowdari[‡]

[†]School of Engineering Sciences and Technology, University of Hyderabad, Gachibowli, Hyderabad 500046, India

[‡]Department of Physics, Advanced Batteries lab, National University of Singapore, Singapore 117542, Singapore

[§]Department of Materials Science and Engineering, National University of Singapore, Singapore 117576, Singapore

Supporting Information

ABSTRACT: Combustion of magnesium in dry ice and a simple subsequent acid treatment step resulted in a MgO-decorated few-layered graphene (FLG) composite that has a specific surface area of 393 m^2/g and an average pore volume of 0.9 cm^3/g. As an anode material in Li-ion batteries, the composite exhibited high reversible capacity and excellent cyclic performance in spite of high first-cycle irreversible capacity loss. A reversible capacity as high as 1052 mAh/g was measured during the first cycle. Even at the end of the 60th cycle, more than 83% of the capacity could be retained. Cyclic voltammetry results indicated pseudocapacitance behavior due to electrochemical absorption and desorption of lithium ions onto graphene. An increase in the capacity has been observed during long-term cycling owing to electrochemical exfoliation of graphene sheets. Owing to its good thermal stability and superior cyclic performance with high reversible capacities, MgO-decked FLG can be an excellent alternative to graphite as an anode material in Li-ion batteries, after suitable modifications.

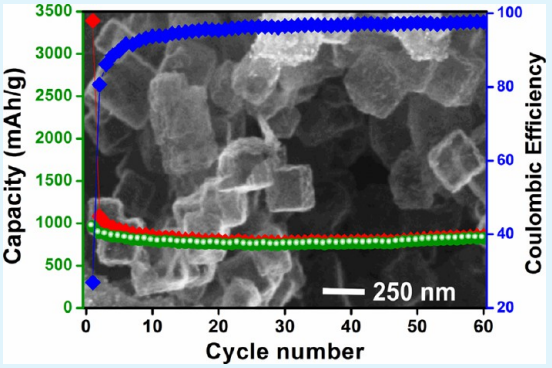

KEYWORDS: *few-layered graphene, MgO, anode, Li-ion batteries, cyclic voltammetry*

1. INTRODUCTION

Graphene has proven its prospective candidature as an anode material in Li-ion batteries (LIBs) in spite of a high initial capacity loss, high voltage hysteresis between discharge and charge plateaus, the potential threat of Li dendrite formation at higher current densities, and the need for improvement in the cyclic performance.[1−5] Even so, owing to graphene's huge lithium storage capability, there is great need to develop new graphene material that should overcome the demerits associated with it as an anode of LIBs. A green and scalable synthesis route that converts dry ice (solid CO_2) to graphene is well practiced.[6] However, according to our knowledge, graphene prepared by this route is not yet studied for anodic application in LIBs. In this route, magnesium (Mg) ribbon is burned in dry ice, resulting in few-layer graphene (FLG) and magnesium oxide (MgO) as the byproducts. Unreacted species and MgO can be removed by treating the sample with concentrated HCl. However, traces of MgO nanoparticles are left as decoration on FLG. Instead of efforts to remove MgO, in this work use of MgO-decorated FLG for anodic application in LIBs has been found to be useful. Trace amounts of MgO may not be a serious issue for the functioning of LIBs because MgO is electrochemically inactive.[7−9] Moreover, its adsorbing and liquid electrolyte retaining capability[10] functions as a protective coating, and its role in enhancing ionic conductivity encourages the use of a MgO-decorated FLG composite as an anode for LIBs.[8,11−15] In addition, the presence of MgO nanoparticles with surface defects may become alternative doping components in FLG, which may be a promising solution to stop the clustering or electroplating and subsequent dendritic growth of Li atoms at the anode of LIBs.[16] We have recently shown the capability of MgO-decorated FLG as an excellent adsorbent to remove SO dye from contaminated water.[17] In this work, the same MgO-decorated FLG is used to make anodes in coin-cell LIBs. The fabricated LIBs are tested for their performance using galvanostatic cycling, cyclic voltammetry (CV), and electrochemical impedance spectroscopy (EIS).

2. EXPERIMENTAL SECTION

2.1. Synthesis. In brief, Mg metal turnings (3 g) were transferred into a circular groove made in a dry ice block. This groove was covered tightly from the top with another dry ice slab immediately when the combustion process started upon ignition of Mg turnings. Combustion results in an ashlike material, which was collected and then dissolved in 1 M HCl and kept for stirring for 24 h. Then the resultant material was filtered and subjected to multiple washes with distilled water. The washing was stopped when the pH of the solution was ~7. The washed

Received: September 20, 2014
Accepted: January 5, 2015
Published: January 5, 2015

DOI: 10.1021/am5064712
ACS Appl. Mater. Interfaces 2015, 7, 2301−2309

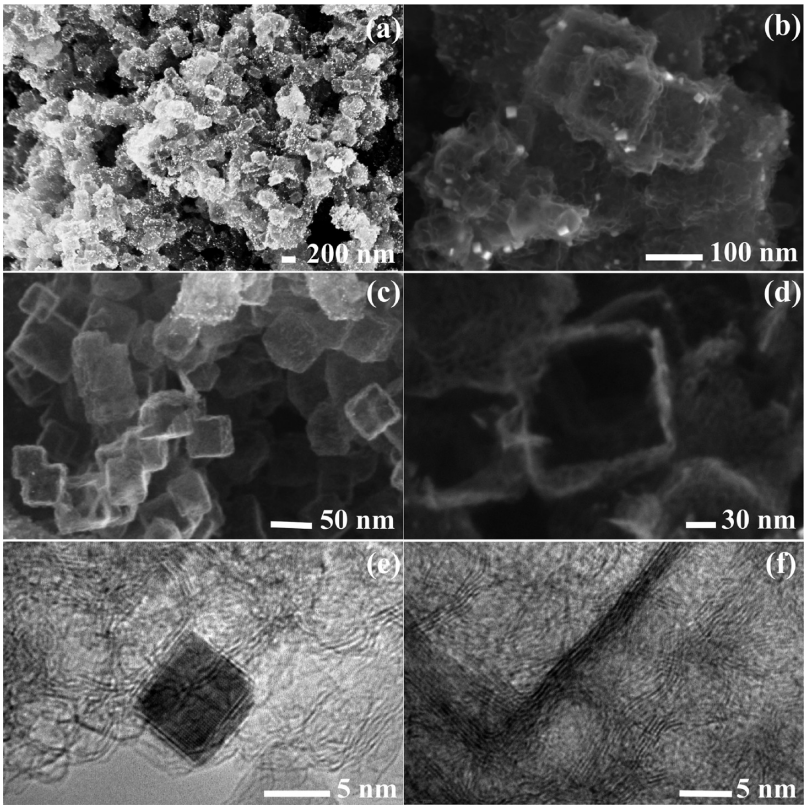

Figure 1. Field-emission scanning electron microscopy images of MgO-decorated FLG (a and b), transparent and semitransparent FLG cubelike features (c and d), and high-resolution TEM (HRTEM) images of a MgO nanoparticle wrapped by bilayered graphene (e) and an edge of the FLG cube (f).

material was filtered and dried in an oven at 100 °C for 12 h. Further synthesis details were reported previously.[17]

2.2. Material Characterization. Morphological studies were carried out by using a transmission electron microscope (model FEI Technai G2 S-Twin) operated at an accelerating voltage of 200 kV. Field emission scanning electron microscope (FESEM) (Model Zeiss Ultra 55) imaging was done at an accelerating voltage of 5 kV. X-ray diffraction (XRD) patterns were recorded from 5 to 80° using Cu Kα radiation as the X-ray source (λ = 1.54 Å); a Philips X'PERT MPD unit, PANalytical system was used to carry out the XRD experiments. A micro-Raman scattering study was carried out using a Renishaw Raman 2000 system. Electron microscopy, XRD, and Raman studies were carried out on as-synthesized and galvanostatic cycled samples to understand the crystallinity and structure of the samples. Specific surface area and porosity details were obtained using Brunauer–Emmett–Teller (BET) formulation by conducting a N_2 physisorption experiment at STP conditions using a Micromeritics Tristar 3000.

2.3. Battery Fabrication. An electrode slurry was made by taking the active material, i.e., MgO-decorated FLG, poly(vinylidene fluoride) (PVDF) binder, and Super P Carbon at 70:15:15 wt % in a *N*-methyl-2-pyrrolidone solvent. After overnight stirring, the slurry was coated onto an etched Cu foil to a thickness of ~25 μm and dried in a hot air oven at 80 °C for 12 h. Then the coated Cu foil was cut into 16 mm-diameter coins, which were dried overnight in a vacuum oven at 80 °C. Coin-type (2016) test cells were fabricated inside a glovebox filled with argon. More details of battery fabrication were discussed in our previous publication.[5] Li metal foil was used as the counter electrode, while a glass microfiber filter (GF/F, Whatman Int. Ltd., Maidstone, England) was used as the separator. 1 M $LiPF_6$ in ethylene carbonate (EC) and dimethyl carbonate (DMC) (1:1 by volume, Merck Selectipur LP40) was used as the electrolyte.

2.4. Electrochemical Characterization. Batteries were tested at room temperature in the voltage range of 0.005–3.0 V by galvanostatic cycling testing at current densities of 37.2 mA/g (0.1 C), 186 mA/g (0.5 C), and 372 mA/g (1.0 C) with a Bitrode battery tester (model SCN; Bitrode Corp., St. Louis, MO), CV at a scan rate of 58 μV/s by MacPile II (Bio-Logic SAS, Claix, France), and impedance studies with an EIS analyzer (model Solartron SI 1260 impedance/gain phase analyzer) in the frequency range of 0.18 MHz–3 MHz with an alternating-current amplitude of 10 mV.

3. RESULTS AND DISCUSSION

The morphology and crystallinity of MgO-decorated FLG has already been discussed.[17] Morphological studies showed that nanosized MgO fragments decorated FLG at several locations. In brief, parts a and b of Figure 1 show the plane-view images of MgO-decorated (bright spots) graphene sheets. Further, semi-transparent and transparent FLG cubelike features with varying sizes are also observed, as shown in Figure 1c,d. Diffraction and Raman scattering analyses showed the presence of MgO and FLG in MgO-decorated FLG. The few-layered nature of the graphene phase is confirmed using Raman and transmission electron microscopy (TEM) analyses. As shown in Figure 3b, the intensity ratio $I_G/I_{2D} \sim 0.7$ corresponds to the number of graphene layers around 6,[18] in agreement with the TEM images of FLG shown in Figure 1e,f. In Figure 1e, the TEM image shows that the MgO nanocube was fully wrapped by transparent bilayer graphene sheets. This observed morphology explains the reason for retention of the MgO nanoparticles even after acid treatment. Recent experimental and theoretical works found that graphene is a perfect insulating membrane to all kinds of chemical species. It will not even allow H^+ ions to pass through its aromatic rings.[19] Thus, graphene acts like a protective coating to MgO and prevents its decomposition by acids like concentrated HCl. Before battery performance tests were conducted, elemental composition (section SI1 in the Supporting Information, SI) of the sample was obtained. It revealed that carbon and MgO are present in 70:30 wt %. This composition is in close agreement with thermogravimetric analysis (TGA) (section SI2 in the SI) in which MgO up to 23 wt % is found. In addition, TGA suggested

DOI: 10.1021/am5064712
ACS Appl. Mater. Interfaces 2015, 7, 2301–2309

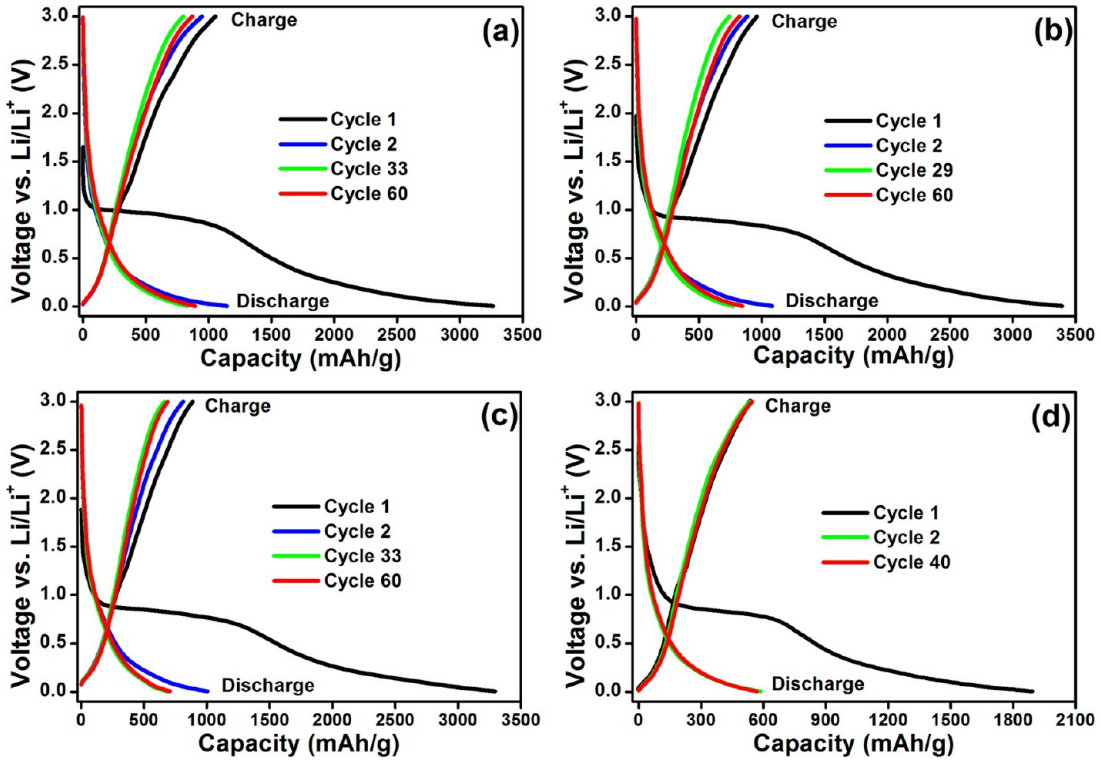

Figure 2. Charge−discharge characteristics of MgO-decorated FLG at current densities of (a) 0.1, (b) 0.5, and (c) 1.0 C. (d) Charge−discharge characteristics of MWCNTs at 0.25 C.

that the sample possesses good thermal stability up to 550 °C even in ambient conditions. The high negative ζ potential value (−49.2 mV at pH ∼ 7; section SI3 in the SI) measured for the sample indicates a strong negative charge on the sample's surfaces. This value is slightly greater than the value of pure graphene materials, and this might result from the presence of negatively charged MgO.[20−22] The high ζ potential value also implies that individual graphene sheets decorated with MgO will show good stability when dispersed in aqueous solutions.[20−22] This will facilitate the easy fabrication of anodes. However, for convenience, these observations are again discussed in this work while comparing them with the observations after battery performance tests.

MgO-decorated FLG shows very stable and similar discharge−charge versus voltage profiles for current rates at 0.1, 0.5, and 1.0 C, as shown in parts a−c of Figure 2, respectively. During the first discharge, irrespective of the current rate, the slope of the curve is consistent up to 1 V, and from there, it changes drastically to form a long plateau region around 0.9−0.7 V that extends up to ∼1350 mAh/g. Further, the discharge curves display a continuous change in the slope until the voltage attains a final set value of 0.005 V. The first and next subsequent charge curves are found to be similar except for a slight decrease in the capacity followed by an increase with an increase in the cycle number. All charge curves are observed to undergo a subtle variation in the slope below 0.5 V and above 2.5 V, while the remaining portion of the curves resembles a straight line. In contrast to the behavior during the first discharge, a long plateau region is not at all observed during the second discharge, while the slope of the curve (below 1.0 V region) continuously changes, similar to the cases of various graphene materials[3,4,23−26] and carbon nanotubes (CNTs)[27−30] (Figure 2d) and their composites.[31] The third and next successive discharge curves are similar to the second discharge curves, and the change of the capacity value is identical with that obtained using charge curves. The large plateau feature observed in the case of MgO-decorated FLG is absent in the case of graphene obtained by various methods in which the slope of first discharge curve changes continuously.[3,4,23−26] This type of characteristic long plateau feature is, however, observed in the case of various kinds of CNTs[27−30] and multiwalled carbon nanotubes (MWCNTs) that are also tested in this work at 0.25 C for comparison purposes and shown in Figure 2d. The initiation of the plateau region around 0.9 V could be ascribed to the formation of a solid electrolyte interphase (SEI), which results from typical initial solvent decomposition wherein Li is irreversibly inserted as covalent compounds like Li_2O, Li_2CO_3, etc.[5,32] This unusually large plateau around 0.9−0.7 V that extends up to very high capacity could be ascribed to high specific surface area and high porosity. Conversion of MgO to the amorphous phase (by enhancing the solvent decomposition on its active surfaces) could also contribute to the above-mentioned large SEI, as indicated by the XRD analysis (Figure 4). The mesopores with large pore volume (∼0.9 cm^3/g) can intake more electrolyte solvent, which eventually decomposes more electrolyte, leading to a large SEI similar to that observed in the case of CNTs.[28]

The specific surface area and porosity distribution that are connected to large SEI formation in the present study are probed with N_2 adsorption and desorption onto fresh MgO-decorated FLG powder followed by BET formulation. A large hysteresis was observed between N_2 adsorption and desorption isotherm curves pertaining to the sample, as shown in Figure 3a, and this type of behavior illustrates the material's high porosity. BET and Langmuir surface areas obtained for the sample are ∼394 ± 2.4 and ∼921 ± 43 m^2/g, respectively. The average pore volume and pore diameter calculated are ∼0.869 cm^3/g and ∼8.82 nm,

DOI: 10.1021/am5064712
ACS Appl. Mater. Interfaces 2015, 7, 2301−2309

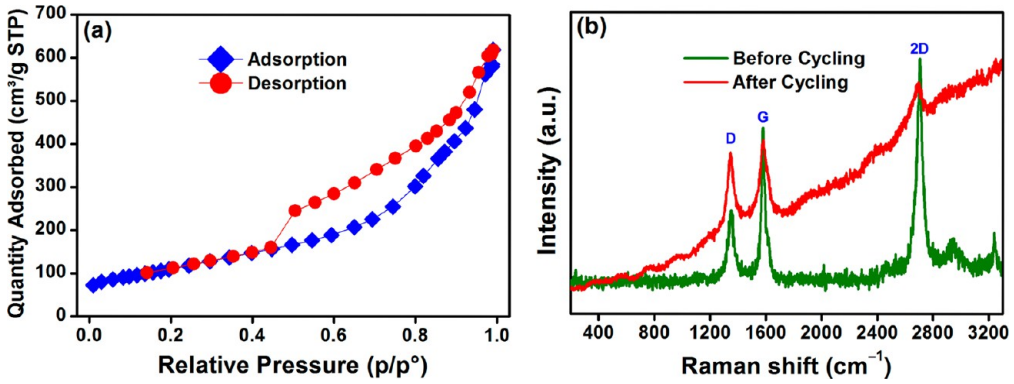

Figure 3. (a) N_2 adsorption and desorption isotherms of MgO-decorated FLG. (b) Raman spectra of MgO-decorated FLG before and after galvanostatic cycling.

respectively. It may not be possible to distinguish the individual contributions of graphene and MgO to the total surface area because both are capable of showing very high specific surface areas; for example, graphene can show a very high experimental value to a theoretical value of 2630 m^2/g,[16,33] while MgO's experimental area is reported in the range of 50−600 m^2/g.[34−37] However, high negative ζ potential and battery testing results in this present study clearly indicate that MgO surfaces contain either a highly catalytic nature or defects that might also lead to this high surface area in addition to the contribution from FLG. Interaction of Li (or electrolyte molecules) with MgO-decorated FLG was also indicated by Raman scattering analysis (Figure 3b). After cycling, the positions of typical Raman bands (D, G, and 2D bands)[9] are found to be unaltered except for the intensity of the G band, which decreased while the 2D band enormously broadened. These observations are indicative of the interaction of Li (or electrolyte molecules) with the active material. The starting material exhibited an intensity (I) ratio I_D/I_G of ∼0.49, which increased to ∼0.92 after 100 cycles of battery testing at 2 C. The increase in the I_D/I_G ratio indicates an increase in the defects or disorder[38] that might be due to the continuous insertion and extraction of Li ions, which eventually increases the interplanar distance between individual graphene sheets. This complimented well with the inferences from diffraction studies on the material after battery testing.

The XRD pattern obtained from the sample after a galvanostatic cycling test is totally different from the original pattern, as shown in Figure 4. The first discharged state pattern showed that most of the MgO crystalline phase converted to amorphous. This conversion might result from decomposition of electrolyte molecules, which consume the oxygen of MgO to form covalent compounds like Li_2O, LiOH, etc., which eventually builds up SEI.[5,32] The observed conversion might be aided by the high-catalytic-natured surface of MgO, and its unique surface chemistry might also play a key role in this conversion.[35] The observed crystal destruction of MgO might be due to loosely bounded edge-sharing oxygen anions, which could be diffused out from MgO by leaving Mg^{2+} ions dispersed in the anode matrix. The observed large unusual SEI, which is absent for various graphene materials referred to this study, might not be possible without MgO's contribution. Now it is clarified that conversion of MgO to amorphous could also be ascribed to large SEI formation in addition to FLG's reducing nature. Moreover, Mg^{2+} ions easily diffuse deep into the anode matrix because their ionic radii are equivalent to those of Li^+ ions and the presence of well-dispersed Mg^{2+} ions is proven to enhance the electrochemical

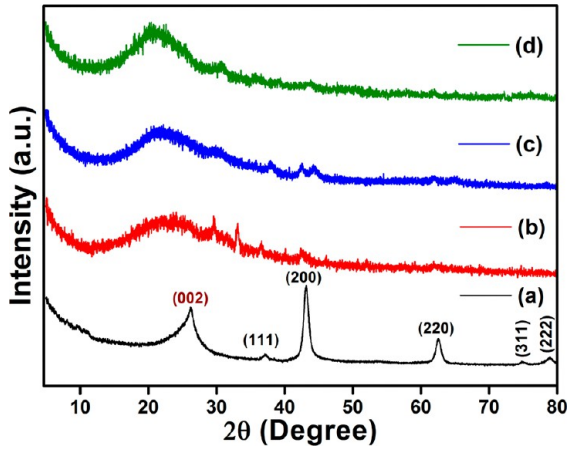

Figure 4. XRD pattern of MgO-decorated FLG: (a) before galvanostatic cycling; (b) after the first discharge to 0.005 V; (c) after the 35th discharge to 0.005 V; (d) after the rate performance test.

properties by improving the electronic and ionic conductivity.[11,13,39,40] The graphitic (002) diffraction peak of fresh MgO-decorated FLG is found at ∼26°, which became very broad and appeared like a hump that centered around 23° after the first discharge. Further shifting and broadening of the graphitic peak toward 20° is observed with an increase in the cycle number, as shown in Figure 4. This broadening and shifting is an indication of an increase in the interplanar distance (d spacing) of graphene sheets. The observed increase in the d spacing plausibly resulted from further exfoliation of graphene sheets due to continuous lithiation and delithiation (electrochemical exfoliation). This observation correlates well with the inferences from Raman scattering and TEM analysis.

Inferences from the XRD and Raman data are further supported by inferences from the electron microscopy results, as shown in Figure 5. After battery testing (Figure 5c,d), MgO is not distinctly observed because of its conversion to a different phase during cycling. An increase in the d spacing in the case of graphene after cycling is also observed. Selected-area electron diffraction (SAED) pattern (Figure 5d) of the sample after cycling clearly indicates the conversion of MgO into a different amorphous phase.

Very high first discharge capacities of around 3295, 3391, and 3261 mAh/g are observed for complete discharge to 0.005 V at 0.1, 0.5, and 1.0 C, respectively. The respective reversible capacities are found to be 1052, 962, and 887 mAh/g during first charge to 3.0 V. Even though Li reversibility is only 28−32%

DOI: 10.1021/am5064712
ACS Appl. Mater. Interfaces 2015, 7, 2301−2309

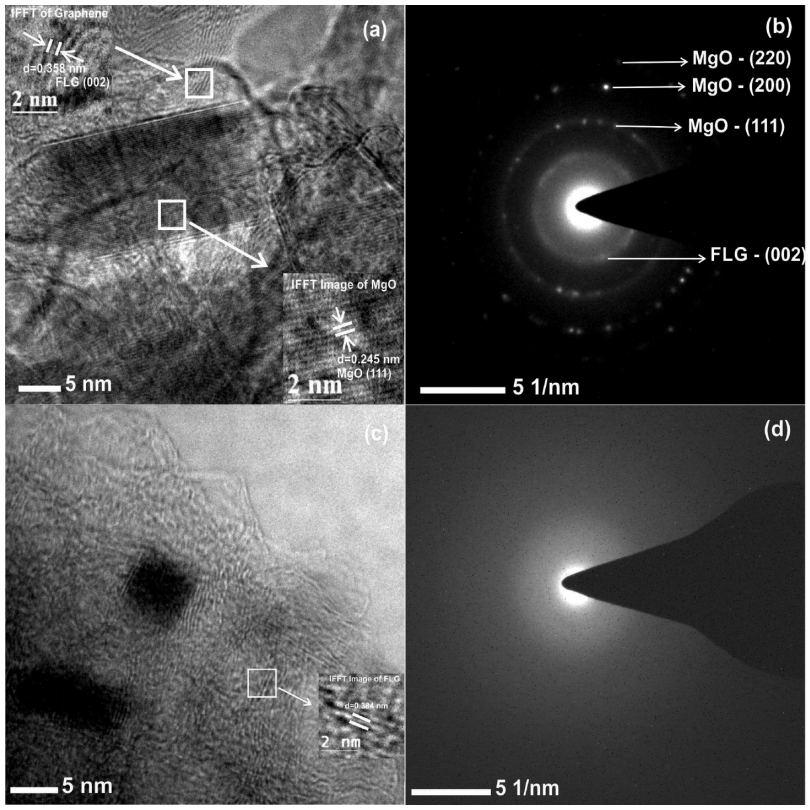

Figure 5. (a) HRTEM image of MgO-decorated FLG with the IFFT image in the inset. (b) SAED pattern of MgO-decorated graphene before cycling. (c) HRTEM image with the IFFT image of FLG in the inset. (d) SAED pattern of FLG after cycling.

during the first cycle, the corresponding capacity value is quite large compared to graphite's theoretical capacity (372 mAh/g). A net 70% capacity loss (about 2200−2300 mAh/g) between the first discharge and charge is considered as the irreversible capacity loss (ICL), which could plausibly result from large SEI like in CNTs[28] along with Li, which covalently bonds with free dangling C atoms at edges and defects of the graphene layers.[41,42] Below 0.5 V, the continuous change in the slope of second and subsequent discharge and charge curves indicates that there is a feeble amount of the Li (de)intercalation type mechanism contributing to the total discharge and charge capacities, while maximum Li storage is credited with electrochemical absorption and desorption complying with CV results (Figure 8).

MgO-decorated FLG as an anode material in LIBs has shown excellent cycling performance, as shown in Figure 6a−c. The respective details are furnished in Table 1. At a low current rate of 0.1 C, a reversible capacity around 1052 mAh/g, which corresponds to the first cycle, fades slowly to 797 mAh/g at the 33rd charge cycle and finally increases to 869 mAh/g at the end of the test. The initial decrease in the capacity can be attributed to long-time solvent decomposition, and an eventual desirable increase might be due to either proper percolation of the electrolyte, which enhances the Li reversibility known as the cycle formation effect,[5] or increases the interplanar distance between graphene sheets, which can create extra active surface area available for additional Li storage.[43] Even Mg^{2+} ion dispersion in the anode matrix, which enhances the electronic and ionic conductivity, could be attributed to the capacity increase, as inferred from XRD results. The Coulombic efficiency (QE) increases randomly in the case of lower current rates, but at higher current rates, it increases constantly. Very low QE values between 26.92 and 32.26% during the first cycle are increased to >82% in the second cycle, soon become >95% after the 16th cycle, and finally reach 97−98% from the 35th cycle onward in all three cases, as shown in Figure 6a−c.

Table 1. Cycling Performance of MgO-Decorated FLG at Various Current Densities

	first cycle			60th cycle			
current rate (C)	DC[a]	CC[b]	QE %	DC	CC	QE %	CR[c]
0.1	3295	1052	32	893	869	97	83
0.5	3391	962	28	850	823	97	86
1.0	3261	887	27	721	703	97	79

[a]Discharge capacity (mAh/g, ±5). [b]Charge capacity (mAh/g, ±5). [c]Capacity retention %.

The rate performance test is carried out with the battery cycled at 1.0 C current rate, as shown in Figure 6d. In this rate capability test, MgO-decorated FLG proved to be an excellent anode material for high current applications because it has shown a reversible capacity of more than 460 mAh/g even at a very high current rate of 5.0 C (1860 mA/g), which is slightly greater than the theoretical capacity of graphite. A significant increase in the capacity is observed after the current rate is changed from high to low, i.e., from 1.0 to 0.1 C and from 5.0 to 0.1 C, as shown in Figure 6d. To further confirm whether this capacity increase is sustained over long-range cycling, the battery that was cycled at 0.5 C is tested at higher current rates starting from 5.0 to 1.0 C, as shown in Figure 7. In this case, the capacity increases by a significant amount to 1619 mAh/g even at 1.0 C at the end of the test. This increase in the capacity might be a result of electrochemical exfoliation of graphene sheets (increased *d* spacing, as

DOI: 10.1021/am5064712
ACS Appl. Mater. Interfaces 2015, 7, 2301−2309

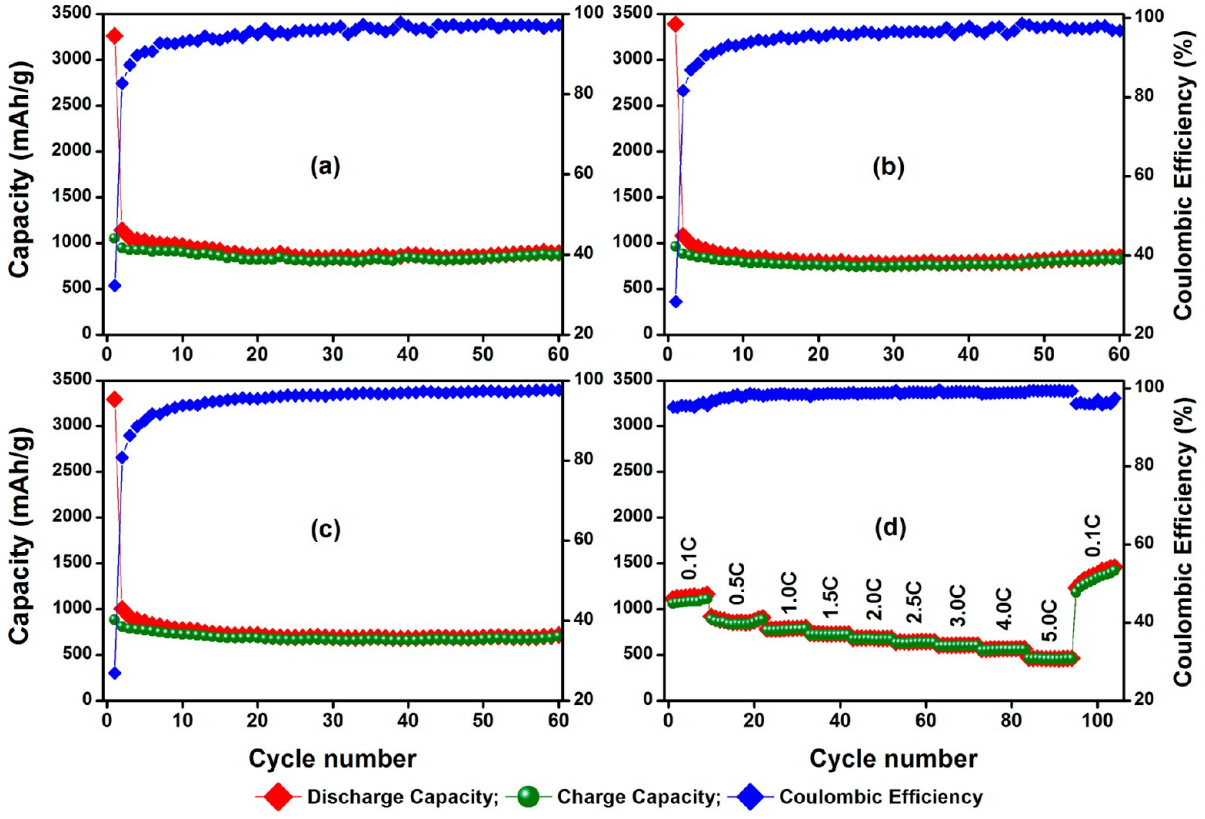

Figure 6. Cyclic performance at (a) 0.1, (b) 0.5, and (c) 1.0 C and (d) rate capability of MgO-decorated FLG.

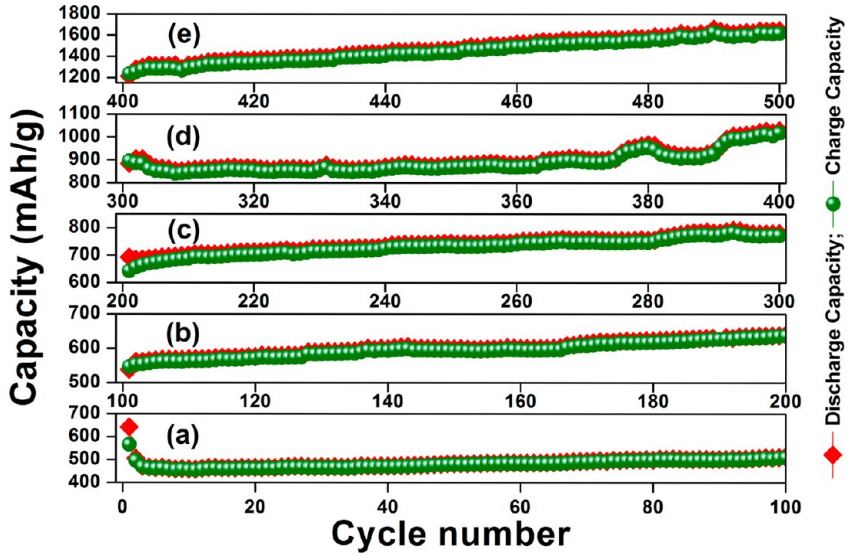

Figure 7. Long-term cycling of MgO-decorated FLG at (a) 5.0, (b) 4.0, (c) 3.0, (d) 2.0, and (e) 1.0 C.

indicated by diffraction and Raman scattering analysis), which seems to be more at higher current rate and capable of bringing extra Li into active traverse between electrodes. Exfoliation of graphene sheets is proven to create additional room (availability of active surface area) for increased Li adsorption onto their surfaces.[43] This kind of increase in the capacity due to volumetric changes caused by exfoliation of graphene sheets was observed in the case of carbon nanofibers[43] upon long-term cycling, but in the case of MgO-decorated FLG, it is observed at a much early stage of aging. Here the surfaces of MgO nanoparticles, which are expected to possess highly catalytic nature, are activated by defects like O^-, O_2^-, etc.,[34] and are expected to avoid Li dendrite formation by decreasing the repulsive interactions between Li−Li ions like electron-deficient dopants do in the case of modified graphene.[16] Thus, MgO nanoparticles also reasonably support the long-time sustainability of anode functioning without failure yet with increased capacity.

The CV results of MgO-decorated FLG for the first six cycles are shown in Figure 8. During first cathodic scan, there are two large reduction current peaks observed at 0.69 V, which corresponds to SEI formation, and at 0.005 V, which relates to cointercalation of the solvated Li ions into FLG.[1] Starting from

DOI: 10.1021/am5064712
ACS Appl. Mater. Interfaces 2015, 7, 2301−2309

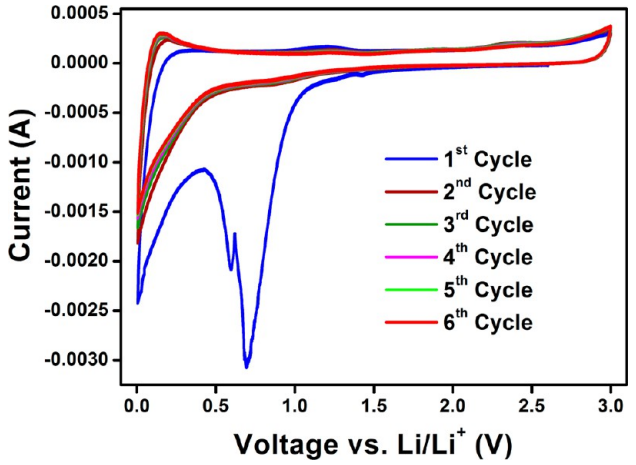

Figure 8. CV results of MgO-decorated FLG.

the very first anodic scan, no significant oxidation current peak is observed, except a small hump around 0.1 V, with a feeble increase in the current. From the second cathodic scan onward, only one reduction current peak is noticed near 0.005 V, which is related to Li insertion into FLG.[1,23] The absence of the large reduction current peak around 0.69 V from the second cycle could be attributed to SEI formation on the electrode surface, which is in good agreement with the large plateau region observed in galvanostatic cycling, which, in turn, results in a high ICL value. The constant redox current at all voltages between 0.5 and 3.0 V might originate as a consequence of fast faradaic reactions taking place on the surface of graphene sheets, i.e., redox currents of Li due to electrochemical absorption and desorption onto graphene planes or defects in it (pseudocapacitance).[2,41,44] From the fourth cycle onward, the decrease in the redox current is negligible and the curves are overlapped strongly with each other, and this can explain the stable capacity behavior of MgO-decorated FLG, as seen in the galvanostatic cycling results. Thus, overall, the absence of a strong redox couple indicates that solid-state intercalation/diffusion of Li is not taking place.[5,45]

The theoretical capacity of graphene varies based on the Li adsorption mechanisms, which are adsorption on both sides[46] of graphene and double-layer formation[47] between two successive graphene sheets, which have a high theoretical capacity of 744 mAh/g. In the case of MgO-decorated FLG, it is ∼1100 mAh/g (at 0.1 C), which is the case of triple-layer formation[48] of Li ions between graphene sheets. Here Li storage at the edges and defects will contribute the least to the capacity because the quality of FLG is very good. The reversible capacity increases to ∼1600 mAh/g at 1 C due to electrochemical exfoliation of FLG. This capacity value suggests that there is a possibility of the formation of four Li-ion layers, the feasibility of which is not yet reported. These unusual Li storage phenomena might take place because of the presence of Mg^{2+} ions, which not only can enhance the electronic and ionic conductivity but also can influence the repulsion between Li−Li ions and thus most plausibly contribute to the stable aforesaid configurations. It is also worth noting that the Mg^{2+} ions are responsible for the prevention of Li electroplating or dendritic growth, which typically leads to the capacity decay. However, this is not the case in the present study. Further robust theoretical studies are needed in order to pinpoint the exact Li storage mechanism and the corresponding voltage range.

EIS is carried out to understand the kinetics of lithiation and delithiation and resistance to charge transfer in MgO-decorated FLG for the first two cycles. The typical Nyquist plot in which semicircles and Warburg line are present is shown in Figure 9 along with the respective equivalent electrical circuits (the values of the circuit elements are shown in section SI4 in the SI). The electrolyte (solution) resistance R_e is found to be ∼1.5−3.5 Ω for various states of the battery (section SI4 in the SI). The resistance to charge transfer R_{ct} is found to be ∼48 Ω at OCV, which increased to ∼94 Ω after the first discharge and once again decreased to ∼59 Ω after the second discharge. However, this value dramatically decreased to ∼8 and ∼6 Ω after the first and second charges, respectively. This observed R_{ct} value is very low compared to the pristine and doped graphene materials reported in the literature.[3,4] This change might be due to the release of Mg^{2+} ions into the anode matrix after the first discharge, which eventually improves the ionic and electronic conductivity. The noticeable decrease in R_{ct} indicates that the faradaic reactions are occurring at a very fast rate and MgO-decorated FLG is partially behaving like an ideal conducting-type electrode (or the battery as a nonpolarizable cell). The value of R_{ct} during the charge process is very low compared that with the discharge, and this observation indicates that Li is desorbing very easily than compared to absorption into the anode matrix. The low value of the intercalation capacity C_i (<1 F) suggests that Li insertion−extraction by intercalation contributes less to the overall capacity, which matches with the observed CV characteristics. The Warburg resistance W_s (resistance to Li-ion diffusion) is found to be relatively higher than R_e and R_{ct}. Thus, the overall low

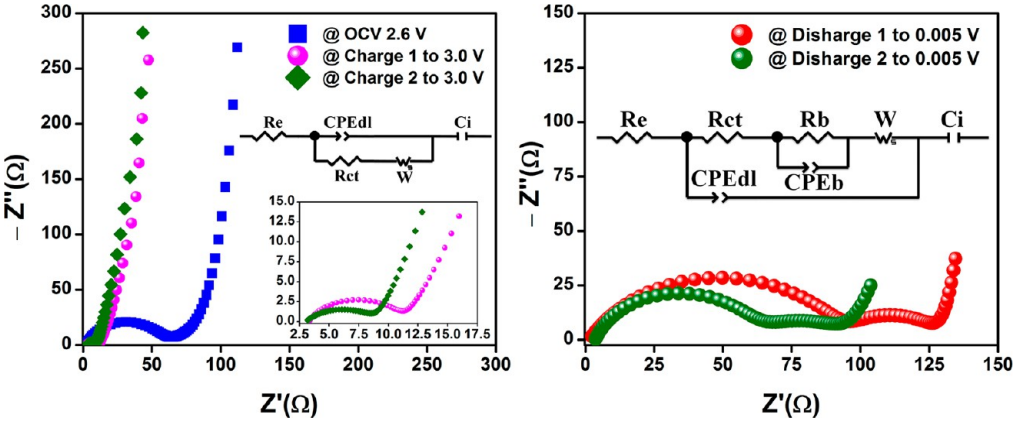

Figure 9. Nyquist plots of MgO-decorated FLG (after fitting) and equivalent circuits of (a) fresh cell, (b) cell discharged to 0.005 V, and (c) cell charged to 3.0 V.

DOI: 10.1021/am5064712
ACS Appl. Mater. Interfaces 2015, 7, 2301−2309

impedance values imply that MgO-decorated FLG is a promising anode material.

4. CONCLUSIONS

MgO-decorated FLG with a high specific surface area and high mesoporosity has been tested as an anode material in LIBs. MgO-decorated FLG has shown a high reversible capacity and excellent constant cyclic performance in spite of the high ICL observed during the first discharge. The QE fluctuated around 98% with a capacity retention of more than 80% even at the 60th cycle. The high ICL value was attributed to electrolyte decomposition due to high specific surface area, porosity, and phase conversion of MgO to amorphous. The electrochemical adsorption and desorption of Li onto graphene (pseudocapacitance) are understood from CV studies. The capacity increase over long-term cycling was mainly ascribed to electrochemical exfoliation of graphene layers, which can create more room to accommodate extra Li. EIS studies confirmed easy lithiation kinetics in the fabricated LIBs and an ideal conducting electrode nature of MgO-decorated FLG. All in all, MgO-decorated FLG was found to exhibit excellent anodic performance and could prevent initial losses upon modification (such as prelithiation) in order to make it commercially viable.

■ ASSOCIATED CONTENT

Supporting Information

Elemental composition (EDS) spectrum of MgO-decorated FLG, ζ potential value of MgO-decorated FLG, TGA of MgO-decorated FLG in air, and EIS table for values of equivalent electrical circuit elements. This material is available free of charge via the Internet at http://pubs.acs.org.

■ AUTHOR INFORMATION

Corresponding Authors

*Tel: +65 6516 2605. E-mail: phymvvr@nus.edu.sg, msemvvr@nus.edu.sg, or reddymvvr@gmail.com.

*Tel: +91 40 2313 4453. E-mail: vvsssse@uohyd.ernet.in.

Author Contributions

The manuscript was written through contributions of all authors. All authors have given approval to the final version of the manuscript.

Notes

The authors declare no competing financial interest.

■ ACKNOWLEDGMENTS

S.P. is grateful to the Government of India for providing financial support through MANF [F1-17.1/2011/MANF-MUS-AND-213/(SA-III/Website)] to pursue a Ph.D. degree at the University of Hyderabad. Due acknowledgement goes to the National University of Singapore (NUS) for providing financial support through an India research initiative (NUS-IRI) fund. N.K.R. is grateful to Government of India for providing financial support through RGNF to pursue a Ph.D. degree at the University of Hyderabad.

■ REFERENCES

(1) Yin, S.; Zhang, Y.; Kong, J.; Zou, C.; Li, C. M.; Lu, X.; Ma, J.; Boey, F. Y. C.; Chen, X. Assembly of Graphene Sheets into Hierarchical Structures for High-Performance Energy Storage. *ACS Nano* **2011**, *5*, 3831−3838.

(2) Jang, B. Z.; Liu, C.; Neff, D.; Yu, Z.; Wang, M. C.; Xiong, W.; Zhamu, A. Graphene Surface-Enabled Lithium Ion-Exchanging Cells: Next-Generation High-Power Energy Storage Devices. *Nano Lett.* **2011**, *11*, 3785−3791.

(3) Zhao, X.; Hayner, C. M.; Kung, M. C.; Kung, H. H. Flexible Holey Graphene Paper Electrodes with Enhanced Rate Capability for Energy Storage Applications. *ACS Nano* **2011**, *5*, 8739−8749.

(4) Wu, Z.-S.; Ren, W.; Xu, L.; Li, F.; Cheng, H.-M. Doped Graphene Sheets As Anode Materials with Superhigh Rate and Large Capacity for Lithium Ion Batteries. *ACS Nano* **2011**, *5*, 5463−5471.

(5) Petnikota, S.; Rotte, N.; Srikanth, V. S. S.; Kota, B. R.; Reddy, M. V.; Loh, K.; Chowdari, B. V. R. Electrochemical Studies of Few-layered Graphene as an Anode Material for Li Ion Batteries. *J. Solid State Electrochem.* **2014**, *18*, 941−949.

(6) Chakrabarti, A.; Lu, J.; Skrabutenas, J. C.; Xu, T.; Xiao, Z.; Maguire, J. A.; Hosmane, N. S. Conversion of Carbon dioxide to Few-Layer Graphene. *J. Mater. Chem.* **2011**, *21*, 9491−9493.

(7) Zhou, W.; Upreti, S.; Whittingham, M. S. High Performance Si/MgO/Graphite Composite as the Anode for Lithium-ion Batteries. *Electrochem. Commun.* **2011**, *13*, 1102−1104.

(8) Wang, Z.; Wu, C.; Liu, L.; Wu, F.; Chen, L.; Huang, X. Electrochemical Evaluation and Structural Characterization of Commercial LiCoO2 Surfaces Modified with MgO for Lithium-Ion Batteries. *J. Electrochem. Soc.* **2002**, *149*, A466−A471.

(9) Chen, J.; Zhao, H.; He, J.; Wang, J. Si/MgO Composite Anodes for Li-ion Batteries. *Rare Met.* **2011**, *30*, 166−169.

(10) Song, M.-S.; Han, S.-C.; Kim, H.-S.; Kim, J.-H.; Kim, K.-T.; Kang, Y.-M.; Ahn, H.-J.; Dou, S. X.; Lee, J.-Y. Effects of Nanosized Adsorbing Material on Electrochemical Properties of Sulfur Cathodes for Li/S Secondary Batteries. *J. Electrochem. Soc.* **2004**, *151*, A791−A795.

(11) Mladenov, M.; Stoyanova, R.; Zhecheva, E.; Vassilev, S. Effect of Mg Doping and MgO-Surface Modification on the Cycling Stability of $LiCoO_2$ Electrodes. *Electrochem. Commun.* **2001**, *3*, 410−416.

(12) Gnanaraj, J. S.; Pol, V. G.; Gedanken, A.; Aurbach, D. Improving the High-Temperature Performance of $LiMn_2O_4$ Spinel Electrodes by Coating the Active Mass with MgO via a Sonochemical Method. *Electrochem. Commun.* **2003**, *5*, 940−945.

(13) Zhao, H.; Gao, L.; Qiu, W.; Zhang, X. Improvement of Electrochemical Stability of $LiCoO_2$ Cathode by a Nano-crystalline Coating. *J. Power Sources* **2004**, *132*, 195−200.

(14) Zhecheva, E.; Mladenov, M.; Stoyanova, R.; Vassilev, S. Coating Technique for Improvement of the Cycling Stability of $LiCoNiO_2$ Electrode Materials. *J. Power Sources* **2006**, *162*, 823−828.

(15) Leo, C. J.; Subba Rao, G. V.; Chowdari, B. V. R. Effect of MgO Addition on the Ionic Conductivity of $LiGe_2(PO_4)_3$ Ceramics. *Solid State Ionics* **2003**, *159*, 357−367.

(16) Liu, Y.; Artyukhov, V. I.; Liu, M.; Harutyunyan, A. R.; Yakobson, B. I. Feasibility of Lithium Storage on Graphene and Its Derivatives. *J. Phys. Chem. Lett.* **2013**, *4*, 1737−1742.

(17) Rotte, N. K.; Yerramala, S.; Boniface, J.; Srikanth, V. V. S. S. Equilibrium and Kinetics of Safranin O Dye Adsorption on MgO Decked Multi-layered Graphene. *Chem. Eng. J.* **2014**, *258*, 412−419.

(18) Das, A.; Chakraborty, B.; Sood, A. K. Raman Spectroscopy of Graphene on Different Substrates and Influence of Defects. *Bull. Mater. Sci.* **2008**, *31*, 579−584.

(19) Berry, V. Impermeability of Graphene and its Applications. *Carbon* **2013**, *62*, 1−10.

(20) Li, D.; Muller, M. B.; Gilje, S.; Kaner, R. B.; Wallace, G. G. Processable Aqueous Dispersions of Graphene Nanosheets. *Nat. Nano* **2008**, *3*, 101−105.

(21) Lotya, M.; Hernandez, Y.; King, P. J.; Smith, R. J.; Nicolosi, V.; Karlsson, L. S.; Blighe, F. M.; De, S.; Wang, Z.; McGovern, I. T.; Duesberg, G. S.; Coleman, J. N. Liquid Phase Production of Graphene by Exfoliation of Graphite in Surfactant/Water Solutions. *J. Am. Chem. Soc.* **2009**, *131*, 3611−3620.

(22) Si, Y.; Samulski, E. T. Synthesis of Water Soluble Graphene. *Nano Lett.* **2008**, *8*, 1679−1682.

(23) Kumar, A.; Reddy, A. L. M.; Mukherjee, A.; Dubey, M.; Zhan, X.; Singh, N.; Ci, L.; Billups, W. E.; Nagurny, J.; Mital, G.; Ajayan, P. M. Direct Synthesis of Lithium-Intercalated Graphene for Electrochemical Energy Storage Application. *ACS Nano* **2011**, *5*, 4345−4349.

DOI: 10.1021/am5064712
ACS Appl. Mater. Interfaces 2015, 7, 2301−2309

(24) Yoo, E.; Kim, J.; Hosono, E.; Zhou, H.-s.; Kudo, T.; Honma, I. Large Reversible Li Storage of Graphene Nanosheet Families for Use in Rechargeable Lithium Ion Batteries. *Nano Lett.* **2008**, *8*, 2277−2282.
(25) Bhardwaj, T.; Antic, A.; Pavan, B.; Barone, V.; Fahlman, B. D. Enhanced Electrochemical Lithium Storage by Graphene Nanoribbons. *J. Am. Chem. Soc.* **2010**, *132*, 12556−12558.
(26) Lian, P.; Zhu, X.; Liang, S.; Li, Z.; Yang, W.; Wang, H. Large Reversible Capacity of High Quality Graphene Sheets as an Anode Material for Lithium-ion Batteries. *Electrochim. Acta* **2010**, *55*, 3909−3914.
(27) Landi, B. J.; Ganter, M. J.; Schauerman, C. M.; Cress, C. D.; Raffaelle, R. P. Lithium Ion Capacity of Single Wall Carbon Nanotube Paper Electrodes. *J. Phys. Chem. C* **2008**, *112*, 7509−7515.
(28) Landi, B. J.; Ganter, M. J.; Cress, C. D.; DiLeo, R. A.; Raffaelle, R. P. Carbon Nanotubes for Lithium Ion Batteries. *Energy Environ. Sci.* **2009**, *2*, 638−654.
(29) Kawasaki, S.; Iwai, Y.; Hirose, M. Electrochemical Lithium Ion Storage Properties of Single-walled Carbon Nanotubes Containing Organic Molecules. *Carbon* **2009**, *47*, 1081−1086.
(30) Landi, B. J.; Dileo, R. A.; Schauerman, C. M.; Cress, C. D.; Ganter, M. J.; Raffaelle, R. P. Multi-Walled Carbon Nanotube Paper Anodes for Lithium Ion Batteries. *J. Nanosci. Nanotechnol.* **2009**, *9*, 3406−3410.
(31) Vinayan, B. P.; Nagar, R.; Raman, V.; Rajalakshmi, N.; Dhathathreyan, K. S.; Ramaprabhu, S. Synthesis of Graphene-Multiwalled Carbon Nanotubes Hybrid Nanostructure by Strengthened Electrostatic Interaction and its Lithium Ion Battery Application. *J. Mater. Chem.* **2012**, *22*, 9949−9956.
(32) Aurbach, D. Review of Selected Electrode−Solution Interactions which Determine the Performance of Li and Li Ion Batteries. *J. Power Sources* **2000**, *89*, 206−218.
(33) Zhu, Y.; Murali, S.; Cai, W.; Li, X.; Suk, J. W.; Potts, J. R.; Ruoff, R. S. Graphene and Graphene Oxide: Synthesis, Properties, and Applications. *Adv. Mater.* **2010**, *22*, 3906−3924.
(34) Sterrer, M.; Diwald, O.; Knözinger, E. Vacancies and Electron Deficient Surface Anions on the Surface of MgO Nanoparticles. *J. Phys. Chem. B* **2000**, *104*, 3601−3607.
(35) Stark, J. V.; Park, D. G.; Lagadic, I.; Klabunde, K. J. Nanoscale Metal Oxide Particles/Clusters as Chemical Reagents. Unique Surface Chemistry on Magnesium Oxide As Shown by Enhanced Adsorption of Acid Gases (Sulfur Dioxide and Carbon Dioxide) and Pressure Dependence. *Chem. Mater.* **1996**, *8*, 1904−1912.
(36) Stoimenov, P. K.; Klinger, R. L.; Marchin, G. L.; Klabunde, K. J. Metal Oxide Nanoparticles as Bactericidal Agents. *Langmuir* **2002**, *18*, 6679−6686.
(37) Bakardjieva, S.; Šubrt, J.; Štengl, V.; Opluštil, F.; Olšanska, M. Magnesium Oxide Nanoparticles as Destructive Sorbent for Toxic Agents. *Microsc. Microanal.* **2004**, *10*, 476−477.
(38) Ferrari, A. C.; Basko, D. M. Raman Spectroscopy as a Versatile Tool for Studying the Properties of Graphene. *Nat. Nano* **2013**, *8*, 235−246.
(39) Wang, B.; Xu, B.; Liu, T.; Liu, P.; Guo, C.; Wang, S.; Wang, Q.; Xiong, Z.; Wang, D.; Zhao, X. S. Mesoporous Carbon-coated $LiFePO_4$ Nanocrystals Co-modified with Graphene and Mg^{2+} Doping as Superior Cathode Materials for Lithium Ion Batteries. *Nanoscale* **2014**, *6*, 986−995.
(40) Yang, Z.; Xia, J.; Zhi, L.; Zhang, W.; Pei, B. An Improved Solid-state Reaction Route to Mg^{2+}-Doped $LiFePO_4$/C Cathode Material for Li-ion Battery. *Ionics* **2014**, *20*, 169−174.
(41) Zhamu, A.; Chen, G.; Liu, C.; Neff, D.; Fang, Q.; Yu, Z.; Xiong, W.; Wang, Y.; Wang, X.; Jang, B. Z. Reviving Rechargeable Lithium Metal Batteries: Enabling Next-Generation High-Energy and High-Power Cells. *Energy Environ. Sci.* **2012**, *5*, 5701−5707.
(42) Sato, K.; Noguchi, M.; Demachi, A.; Oki, N.; Endo, M. A Mechanism of Lithium Storage in Disordered Carbons. *Science* **1994**, *264*, 556−558.
(43) Wu, Y.; Reddy, M. V.; Chowdari, B. V. R.; Ramakrishna, S. Long-Term Cycling Studies on Electrospun Carbon Nanofibers as Anode Material for Lithium Ion Batteries. *ACS Appl. Mater. Interfaces* **2013**, *5*, 12175−12184.
(44) Simon, P.; Gogotsi, Y. Materials for Electrochemical Capacitors. *Nat. Mater.* **2008**, *7*, 845−854.
(45) Nazri, G. A.; Pistoia, G. *Lithium Batteries: Science and Technology*; Springer: Berlin, 2009.
(46) Lee, E.; Persson, K. A. Li Absorption and Intercalation in Single Layer Graphene and Few Layer Graphene by First Principles. *Nano Lett.* **2012**, *12*, 4624−4628.
(47) Suzuki, T.; Hasegawa, T.; Mukai, S. R.; Tamon, H. A Theoretical Study on Storage States of Li Ions in Carbon Anodes of Li Ion Batteries using Molecular Orbital Calculations. *Carbon* **2003**, *41*, 1933−1939.
(48) Chan, Y.; Hill, J. Lithium Ion Storage between Graphenes. *Nanoscale Res. Lett.* **2011**, *6*, 203.

DOI: 10.1021/am5064712
ACS Appl. Mater. Interfaces 2015, 7, 2301−2309